Engineering Failure Analysis 96 (2019) 31–43

Contents lists available at ScienceDirect

Engineering Failure Analysis

journal homepage: www.elsevier.com/locate/engfailanal

Failure analysis of an un-anchored steel oil tank damaged during the Silakhor earthquake of 2006 in Iran

Sina Miladi, Mehran S. Razzaghi*

Department of Civil Engineering, Qazvin Branch, Islamic Azad University, Qazvin, Iran

ARTICLE INFO

Keywords:
Seismic performance
Unanchored tank
Buckling, uplift
Failure analysis

ABSTRACT

On March 31, 2006, a destructive earthquake (M_w = 6.1) occurred in western Iran. Because of the earthquake, some of the old un-anchored cylindrical steel fuel storage tanks were damaged. The damaged tanks experienced the horizontal peak ground acceleration (PGA) of 0.44g. During the earthquake, the most affected tank experienced shell uplift. Because of the tank-to-foundation impact, the concrete cover of the tank foundation was damaged. In addition, the evidences of slight buckling were observable on tank shell. In this study, failure analysis was performed on the most affected tank. In order to evaluate the seismic performance of the studied tank, existing analytical relations were carried out as well as the inelastic response history analysis. To this end, the accelerogram of the recorded earthquake at a station close to the selected tank was used. Numerical analysis was performed using ABAQUS software. In addition, a parametric study was carried out to evaluate the effect of amount of stored liquid on seismic behavior and performance of the studied tank. Results of this study revealed that the numerical model is capable of estimating the actual performance of the tank. It was shown that the critical PGA of the dynamic buckling of the considered tank is 0.285g. Additionally, the uplift threshold PGA is 0.23g.

1. Introduction

Aboveground cylindrical steel tanks play an important role in storing various types of liquid in chemical industries, especially in refineries and petrochemical plants. Inappropriate performance of tanks, specially unanchored tanks, in previous earthquakes, including Anchorage (Alaska) earthquake in 1964, Izmit (Turkey) seismic event in 1999 and Bam (Iran) earthquake in 2003 indicated the seismic vulnerability of such structures [1–5]. In many process industries, tanks store a remarkable volume of flammable and toxic materials. Hence, damage to such structures may causes environmental pollution, fire disasters and work abandon in addition to physical losses. For instance, in the 1999 Izmit earthquake, a number of tanks in the Tupras refinery were burned. Due to spread of fire, the wooden cooling tower of the refinery was completely burned [6]. Furthermore, in Niigata earthquake of 1964 in Japan, ignition of six petroleum tanks in an oil refinery caused burning of more than 250 neighboring houses [7].

Because of the importance of the acceptable performance of the tanks during earthquakes, various researchers have focused on evaluation of seismic performance of such structures [5,8]. Researches showed that, during an earthquake, the upper parts of the liquid, so-called the convective liquid, move in a long period motion. Meanwhile, the lower parts experience high-frequency motions. The later part of liquid is known as impulsive liquid [9]. The dynamic response of the liquid to the earthquake causes overturning moment at the tank bottom. In anchored tanks, the overturning moment may causes tension of mechanical anchors. While, in unanchored tanks, shell uplift may happens due to the overturning moment. Since the uplifting response of the tank is geometrically

* Corresponding author at: Department of Civil Engineering, Qazvin Branch, Islamic Azad University, Nokhbegan Blvd., Qazvin, Iran.
E-mail address: razzaghi.m@gmail.com (M. S. Razzaghi).

https://doi.org/10.1016/j.engfailanal.2018.09.031
Received 2 June 2018; Received in revised form 17 September 2018; Accepted 24 September 2018
Available online 26 September 2018
1350-6307/

nonlinear, the seismic behaviors of unanchored tanks are remarkably complex [5,10]. Although, uplift cannot be considered as a damage itself, it can cause significant damages; such as shell buckling, rupture of pipes connected to the tank and damage to foundation. Previous studies and performances of unanchored tanks during occurred earthquakes revealed that these tanks are more vulnerable than mechanically anchored ones [11]. The complex behavior of unanchored liquid storage tanks, their significant seismic vulnerability and remarkable direct and indirect consequences of their inappropriate performance, enhance the necessity of evaluation of the seismic performance of these structures.

Investigating the performances of structures during happened earthquakes is an important approach to perceive the seismic performance of structures. In other words, seismic events can be considered as full-scale experiments to study the seismic behavior of structures. Therefore, in order to get a better idea about dynamic performance of a particular complex structure, such as an unanchored tank, numerical analysis can be employed to simulate the actual performance of the structure to a happened earthquake. In such a case, causes of structural failures can be investigated by interpreting the results of numerical analysis and comparing the numerical results with actual performance of the structure during the occurred earthquake.

This study focuses on failure analysis of an unanchored liquid storage tank subjected to the Silakhor earthquake of 2006 in Iran. To this end, the behavior and seismic performance of the damaged tank was evaluated using analytical relations and numerical nonlinear response history analyses. Results of numerical dynamic analyses and analytical relations were compared with actual performance of the damaged tank during the earthquake.

2. Description of the event

On March 31, 2006, an earthquake of M_w = 6.1 occurred in Silakhor in western Iran. The earthquake was occurred at 33.56°N 48.73°E, at a focal depth of 7 kms [12]. The focal mechanism of the earthquake was strike-slip. The maximum PGAs were recorded at Chalanchulan strong ground motion station (4.32 m/s^2 and 5.24 m/s^2 for horizontal and vertical component respectively) [12]. The recorded accelerograms of the earthquake and its response spectra are shown in Figs. 1 and 2 respectively.

Due to the earthquake, urban and rural areas were widely damaged. Moreover, the earthquake caused failure of many industrial facilities in the affected area. At least 28 on-ground cylindrical tanks experienced earthquake. As listed in Table 1, twenty-five of the tanks were unanchored and three were mechanically anchored.

During the earthquake, none of the anchored tanks was damaged. Meanwhile, 75% of unanchored tanks, which were located at sites with epicentral distances of 5 km or less experienced minor to moderate damages. As mentioned in Table 1, the evidence of shell uplift were observed in all damaged tanks. It should be noted that 70% of the undamaged unanchored tanks were completely empty.

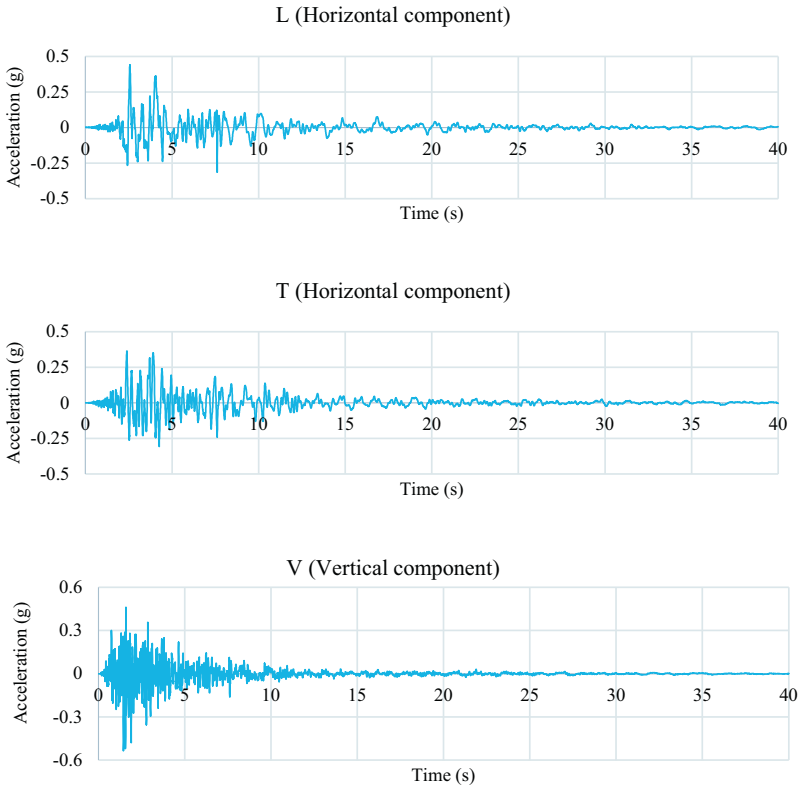

Fig. 1. Acceleration time-history of the Silakhor earthquake components record at chalanchulan station.

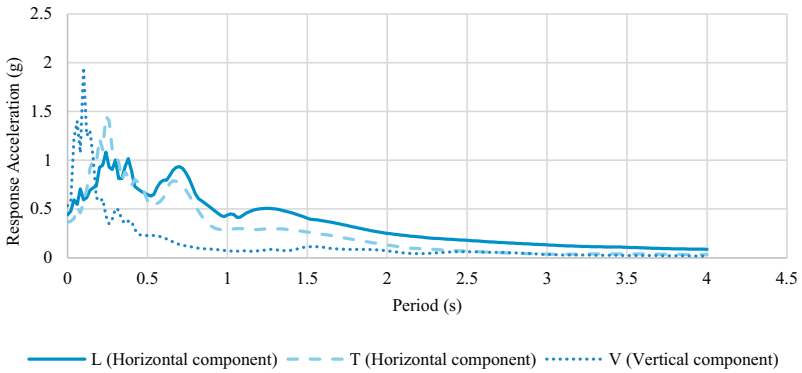

Fig. 2. Response spectra of the Silakhor earthquake components record at chalanchulan station.

Table 1
Specifications of observed tanks following the Silakhor earthquake.

Tank Identification	Quality	H/D	Roof Type	Anchorage	Liquid	Percentage (%) full	L (km)	Damage	Description Of Damage
T1	1	0.55	Fixed	Un-anchored	Fuel Oil	0.91	<5	Minor	Shell uplift- Fracture of isolation layer of pipes- Roof of wrinkling
T2	1	0.55	Fixed	Un-anchored	Fuel Oil	0.92	<5	Minor	shell uplift- Fracture of isolation layer of pipes- Leakage of oil from bottom plate
T3	1	1.2	Fixed	Un-anchored	Fuel Oil	0.87	<5	Moderate	Shell uplift- Cracking of foundation- Buckling
T4	2	1.2	Fixed	Un-anchored	Molasses	0.9	<5	No Damage	–
T5	2	1.2	Fixed	Anchored	Molasses	0.3	<5	No Damage	–
T6	1	1.3	Fixed	Anchored	Gas-Oil	Unknown	<5	No Damage	–
T7	1	1.6	Fixed	Un-anchored	–	0	10	No Damage	–
T8	2	2	Fixed	Un-anchored	–	0	10	No Damage	–
T9	1	1.2	Fixed	Un-anchored	–	0	10	No Damage	–
T10	2	1.2	Fixed	Un-anchored	–	0	10	No Damage	–
T11	6	1.5	Fixed	Un-anchored	–	0	10	No Damage	–
T12	1	0.37	Fixed	Un-anchored	Oil	0.12	>20	No Damage	–
T13	1	0.37	Fixed	Un-anchored	Gas-Oil	0.64	>20	No Damage	–
T14	1	0.5	Floating	Un-anchored	Oil	0.21	>20	No Damage	–
T15	1	0.5	Floating	Un-anchored	Gasoline	0.55	>20	No Damage	–
T16	1	0.5	Floating	Un-anchored	Oil	0.15	>20	No Damage	–
T17	1	0.5	Floating	Un-anchored	Oil	0.15	>20	No Damage	–
T18	1	0.8	Fixed	Un-anchored	Lubricant	0	>20	No Damage	–
T19	1	0.8	Fixed	Un-anchored	Lubricant	0	>20	No Damage	–

Besides, all of the damaged tanks experienced peak ground accelerations about 0.4 g.

3. Field investigation of the studied tanks

The most affected tank among all of the observed tanks is T3 (See Table 1). Accordingly, in this study, the failure analysis of the T3 tank was performed. The tank was located in an industrial plant in Chalanchulan region, very close to the strong ground motion station.

The considered tank is an unanchored cylindrical steel tank rested on a reinforced concrete foundation. The tank has a conical fixed roof. The tank shell contains three strakes of the same thicknesses. Strakes are made of curved panels interconnected using groove welds. The content of the tank was fuel oil and during the earthquake, it was about 90% full. The tank is very old and therefore, it was not designed according to seismic design codes. It should be noted that the height-to-diameter ratio (H/D) of the tank is 1.2. The geometric specifications of the tank are shown in Fig. 3.

Following the earthquake, the concrete cover of foundation was cracked (See Fig. 4a). The reason of such a failure would be significant shell uplift and collision of the uplifted tank with its foundation.

In addition, as shown in Fig. 4b the tank shell experienced buckling during the earthquake. The buckling was observable in the middle of the lowest strake of the shell. It should be noted that the orientation of the shell buckled portion and cracked area of foundation were the same. Thus, it seems that the shell buckling happened above the most uplifted zone of the tank bottom.

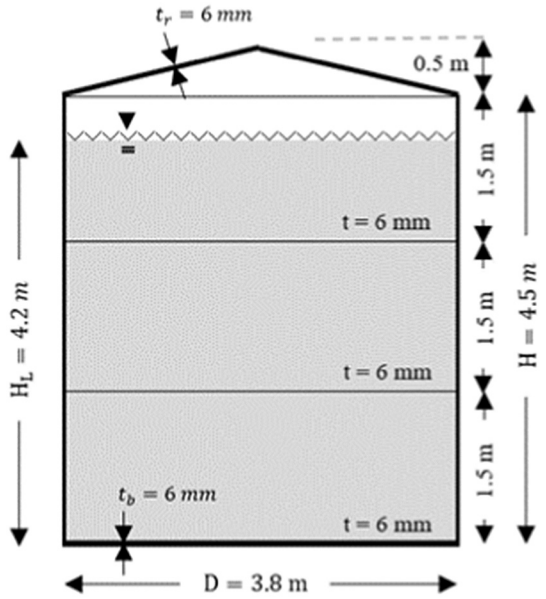

Fig. 3. Geometric specifications of T3 tank (t is the shell thickness).

4. Failure analysis

In order to assess the seismic performance of T3 tank during the Silakhor earthquake, nonlinear response history method was employed. To this end, the accelerogram recorded in Chalanchulan strong ground motion station was used. Herein two numerical approaches were followed: response history analysis using the natural earthquake record and the incremental dynamic analysis (IDA) using scaled earthquake records. Finite element modeling and analyzing of the tank was carried out using ABAQUS software [13].

4.1. Shell, roof and bottom plate modeling

For modeling the different structural components of the tank, S4R shell elements were used. This element has four nodes having six degrees of freedom at each node, including three translational and three rotational degrees of freedom. This element is capable of considering large displacements and nonlinear behavior of the structural material and therefore is appropriate for solving the inelastic buckling problems. A bilinear model was employed for considering the material properties of steel (See Table 2). The steel nonlinearity were accounted for based on Von Mises yield criteria considering kinematic hardening rule. The large deformation effects were considered during the analyses. The FEM mesh of structural components of the tank is indicated in Fig. 5.

4.2. Liquid modeling

There are several methods to consider the effect of fluid-structure interaction during an earthquake including finite element method using Eulerian, Lagrangian and Eulerian-Lagrangian fluid elements and boundary element methods. Furthermore, added mass method has been also implemented by several researchers. All of the abovementioned methods has their own advantages and shortcomings. They have been implemented by various researchers considering their benefits and drawbacks for a particular study [14-17].

In this study, the added mass method has been used. The added mass method was proposed by Westergaard [18] for modeling the effect of fluid-structure interaction in dams. This method is consistent with large displacement FEM analyses and thus, it would be beneficial for solving tank buckling problems. It has an acceptable convergence rate and requires less calculation time comparing to other methods.

In this method, the effect of liquid is obtained through the addition of effective liquid mass on the tank shell. Variation of the added mass in different parts of the shell are obtained from the hydrodynamic pressure distribution of the impulsive liquid. The impulsive pressure at each point of the tank circumference is a function of its distance from the bottom of the tank and the angle between that point and the direction of lateral ground acceleration [15]:

$$P_i(\eta, \theta, t) = C_i(\eta).\ \rho.\ \ddot{x}_g(t).\ \cos\theta \tag{1}$$

Where $C_i(\eta)$ is the impulsive pressure distribution along the cylinder's height in accordance with Eq. 2, and $\eta = z/H_L$; z is the distance between the circumferential nodes and tank bottom and H_L is the height of liquid.

(a)

(b)

Fig. 4. Damages observed in the T3 tank a) cracked foundation of the tank b) slight buckling of the shell.

Table 2
Material Properties of Steel and Contained Liquid.

Material	Density Kg/m^3	Elasticity Modulus GPa	Tangent Modulus MPa	Yield stress MPa	Poisson ratio
Steel	7850	210	4×10^3	240	0.3
Fluid	920	–	–	–	–

$$C_i(\eta) = 1 - \sum_{n=1}^{\infty} C_{cn}(\eta) \tag{2}$$

The function $C_{cn}(\eta)$ is the convective pressure distribution along the cylinder's height, which can be calculated using Eq. 3.

$$C_{cn}(\eta) = \frac{2}{\lambda_n - 1} \frac{\cos h\left[\lambda_n \left(H_L/R\right) \eta\right]}{\cos h\left[\lambda_n \left(H_L/R\right)\right]} \tag{3}$$

Where R is the tank radius and λ_n is the nth root of the Bessel function. Usually, using the first three roots of the Bessel function ($\lambda_1 = 1.841$, $\lambda_2 = 5.311$, $\lambda_3 = 8.536$) are sufficient to achieve appropriate results [15].

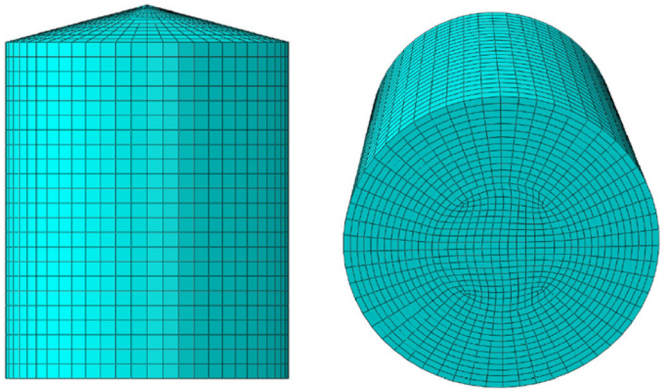

Fig. 5. FEM mesh of the tank shell, roof and bottom plate.

To determine the lumped mass at the surface of the liquid and the bottom nodes of the shell the Eq. 4 can be used, whereas the Eq. 5 can be used to calculate the lump mass m_i for an interior node (See Fig. 6):

$$m_{i'} = \frac{P_{i'}}{2}\frac{\Delta h}{a_n} \tag{4}$$

$$m_i = P_i\frac{\Delta h}{a_n} \tag{5}$$

$P_{i'}$ is the impulsive pressures applied to the point i' which located at the surface of liquid or the tank bottom, P_i is the impulsive pressure at the interior point i, Δh is the distance between the adjacent nodes in vertical direction and a_n is the reference normal acceleration which can be calculated as follows:

$$a_n = \ddot{x}_g(t).\cos\theta \tag{6}$$

Where, $\ddot{x}_g(t)$ is the earthquake acceleration time history and θ is the circumferential position. The distribution of $C_i(\eta)$ along the tank height for the T3 tank is shown in Fig. 7.

The added masses were modeled using mass elements. The mass elements were connected to the nodes of S4R shell elements by massless rigid links. To this end, MPC type LINKs were employed to constrain mass elements to corresponding shell nodes. As indicated in Fig. 8, the MPC links are restrained with supports, oriented in their local axes. The movement of the support is restricted in the vertical as well as the tangential (perpendicular) direction. However, it is free to move in the local axial direction (i.e. the global radial direction). Hence, the nodal masses are allowed to move only in the direction normal to the shell.

4.3. Uplift modeling

Unanchored tanks may encounter uplift due to the seismic excitation. ABAQUS software is capable of modeling the contact and separation of bottom plate and foundation. There are several methods in the software that can consider and analyze contacts and impact. In this study surface-to-surface contact interactions were used. This method can model contact between two flexible surfaces or between a flexible surface and a rigid one [13].

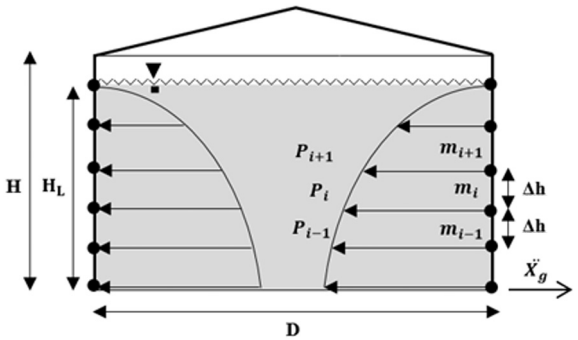

Fig. 6. Variation of the added mass along the shell height.

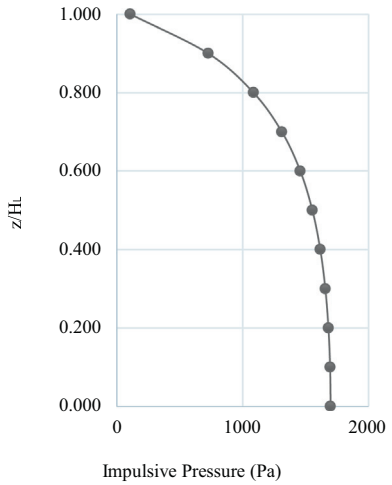

Fig. 7. Variation of impulsive pressure along the T3 tank shell.

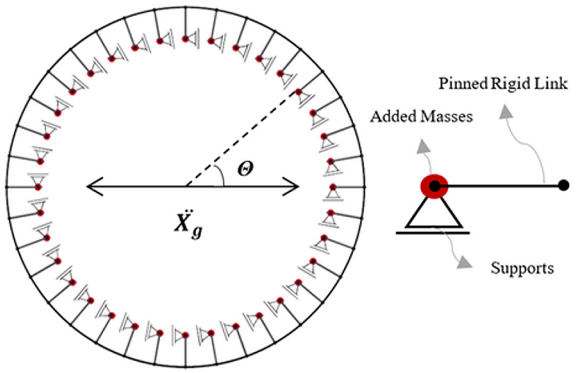

Fig. 8. A schematic of added mass model.

5. Evaluation of dynamic buckling

Shell buckling is one of the most common failure mechanisms in cylindrical steel tanks, especially unanchored ones. As shown in Fig. 4b, a distortion was observable on tank surface. In order to evaluate the buckling in the studied tank, two approaches (using analytical relations and determining the critical PGA using IDA) were carried out.

5.1. Using analytical relations

One of the most widely used analytical relations for calculating the buckling capacity of tanks is Rotter's relation [19]. This relation has been used as a of elastic-plastic buckling criterion in various guidelines and codes, including the design guidelines for the New Zealand National Society for Earthquake Engineering (NZSEE) [20] and Eurocode8 [21]. The inelastic buckling capacity of the tank shell σ can be calculated as follows:

$$\sigma = \sigma_{cl}\left\{1-\left(\frac{P.R}{F_y.t}\right)^2\right\}\left\{1-\frac{1}{1.12+\rho^{1.5}}\right\}\left\{\frac{\frac{F_y}{250}+\rho}{1+\rho}\right\} \tag{7}$$

Where $\rho = \frac{R/t}{400}$, R is the tank radius, P is the total internal pressure and F_y is the steel yielding stress. σ_{cl} is the classical elastic critical stress in a cylindrical shell, obtained from the relation $\sigma_{cl} = 0.605\frac{E.t}{R}$ for steel shells. Where, E and t are the elastic modulus and the thickness of the tank shell, respectively.

By substituting the specifications of T3 tank in Eq. 7, the elastic-plastic buckling capacity of 170 *MPa* is calculated for the tank.

In order to estimate the stresses created in the tank shell during the Silakhor earthquake, nonlinear response history analysis was performed using the acceleration time history of the earthquake recorded at Chalanchulan station. Accordingly, by comparing the maximum axial compression of the shell with its buckling capacity calculated by Eq. 7, the occurrence of buckling in tank shell can be investigated.

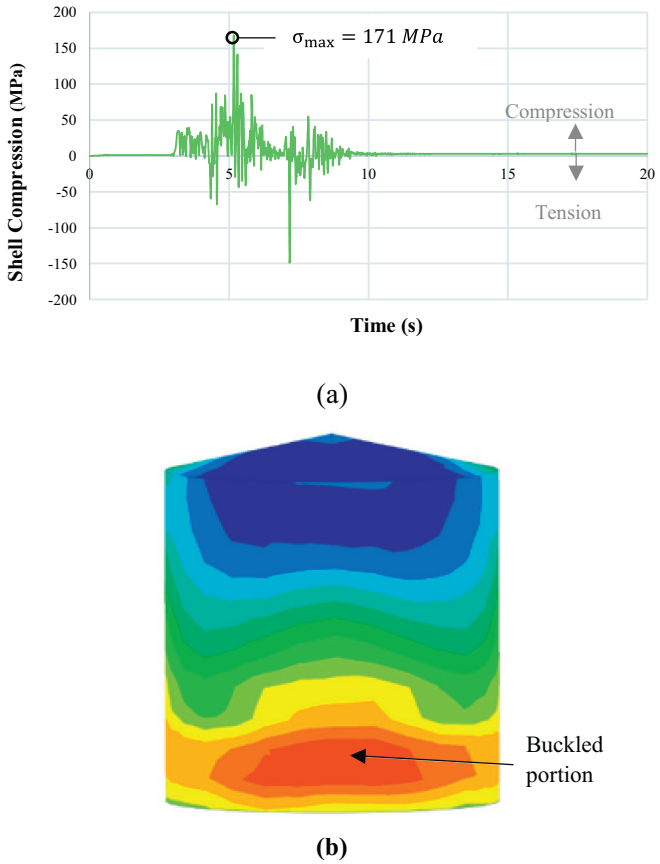

Fig. 9. Results of the response history analysis
a) Time history of the shell axial stress b) Distribution of the axial stress at the beginning of buckling.

Fig. 9a shows the time history of axial compression stress of T3 tank during the earthquake. As shown in this Figure, the maximum axial compression stress of the shell is slightly greater than the shell's buckling capacity, which indicates that the buckling has been happened in the tank shell during Silakhor earthquake. Fig. 9a also indicates that the buckling occurs after the fifth second of the earthquake. It should be noted that as indicated in Fig. 9b, according to the results of numerical analysis the maximum shell stress was created in the middle of the lowest shell strake, which is consistent with the actual performance of the tanks observed during the field investigation.

5.2. Numerical analysis

Existing analytical relations for evaluating shell buckling are generally based on Quasi-Static approach and may be different from the actual seismic performance of tanks to some extent. Therefore, dynamic methods usually result in more reliable estimates for buckling capacity of tank shells. In order to determine the critical load for dynamic buckling of shells, the Budiansky–Roth method [22,23] can be used. This method has been used by various researchers to calculate the critical buckling load [24–26]. This method is based on the incremental dynamic analysis (IDA) of a particular structure under a specific input motion. In other words, different ranges of a specific record with sufficiently small steps of PGA is applied to the tank and the PGA which make a jump in the radial displacement of the shell is determined as the critical PGA (PGA_{cr}). The time history of the radial displacement of the studied tank shell is shown in Fig. 10. The Pseudo-equilibrium path is usually used for recognizing the PGA_{cr} [25].

To this end, the maximum radial displacement of the shell should be plotted in terms of PGA. Due to the slope variation of shell radial displacement after the buckling, the illustrated points will show two different paths. By using linear regression, these two paths can be specified in two recognizable lines. The PGA corresponding to the intersection point of these two lines represents the PGA_{cr}. The Pseudo-equilibrium path for the studied tank under the Silakhor scaled earthquake is shown in Fig. 11. As shown in this Figure, the PGA_{cr} is equal to 0.285g.

Since the occurred earthquake has a maximum acceleration of 0.44g, it can be concluded that during the Silakhor earthquake, the buckling has been occurred in the tank shell. It is evident that the maximum radial displacement of the shell would happen in the buckled area. In the studied tank, the maximum radial displacement was observed in the middle parts of the lowest strake. As previously described this results is consistent with actual performance of the damaged tank.

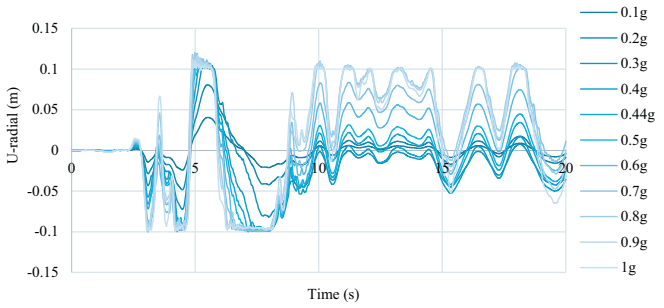

Fig. 10. Time histories of the maximum radial displacement of the finite element model for various PGAs.

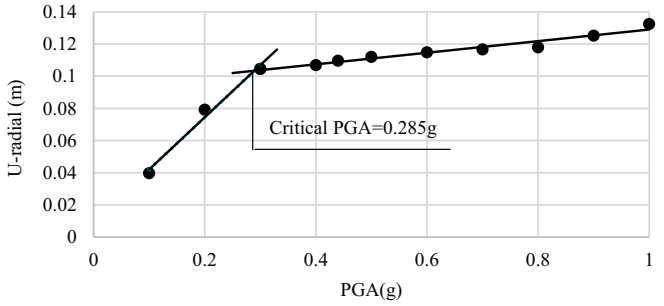

Fig. 11. Pseudo-equilibrium path for critical node of the finite element model.

6. Evaluation of tank uplift

Tank uplift is a probable behavior in every un-anchored tank. Such a behavior has occurred in many tanks during previous earthquakes. Performance of the uplifted tanks is highly dependent to the severity of uplift. Because of the importance of tank uplift, several researchers have presented analytical models and relations for evaluating uplift [9,10 and 27].

As shown in Fig. 4, the evidence of occurring uplift in T3 tank was clearly observed during the field investigations. In order to investigate the uplift in the studied tank two methods were used: using the analytical relations and nonlinear response history analysis.

6.1. Using analytical relations

In order to estimate the maximum probable uplift of the studied tank, the modified Cambra's expression, which is provided by NZSEE [20] were used. Based on the above-mentioned method, the maximum uplift can be calculated as follows:

$$\nu = \frac{1}{C}\left[\frac{f_{yb}\, t_b^2}{6\, N_x} + \frac{p_0\, L_b}{N_x}\left[\frac{L_b}{2} - \left(\frac{E\, t_b^3}{12\, N_x}\right)^{1/2}\right]\right] \tag{8}$$

where $N_x = f_{rb}t_b$, $L_b = 2R(1-\tau)$, $\tau = \frac{r}{R}$, $f_{rb} = \frac{1}{t_b}\left[\frac{2Et_b\, p_0^2 R^2 (1-\tau)^2}{3}\right]^{1/3}$, f_{yb} is the yield stress in the base plate material, C is a foundation stiffness factor (equal to 1.0 for stiff foundations), r is the radius of the area of bottom plate that does not uplift. t_b is the thickness of base plate, p_0 is the hydrostatic pressure over the base and f_{rb} is the membrane stress in bottom plate.

Using relation 8 requires consideration of the initial assumption for the radius of unuplifted area (r) and also recurrent calculations. The recurrent calculations should be continued until obtaining the equal resistant and overturning moments. By substituting the specifications of T3 tank in Eq. 8 the uplift value of 10 mm is estimated for the inspected tank.

6.2. Dynamic analysis

Available analytical relations presented to estimate tank uplift are based on quasi-static method. In order to achieve a more precise estimation of uplift response of the tank during the happened earthquake, nonlinear response history analysis should be implemented. The results of numerical analysis of the studied tank using the Silakhor earthquake record is illustrated in Fig. 12. As shown in this Figure, the maximum tank uplift is 40*mm*, which is remarkably greater than the results of Cambra's model. This uplift occurred shortly before the fifth second of the earthquake. As described in section 5.1, the shell buckling approximately happened at the fifth second of the earthquake. In other words, the shell buckling happened just after the maximum vertical displacement of the

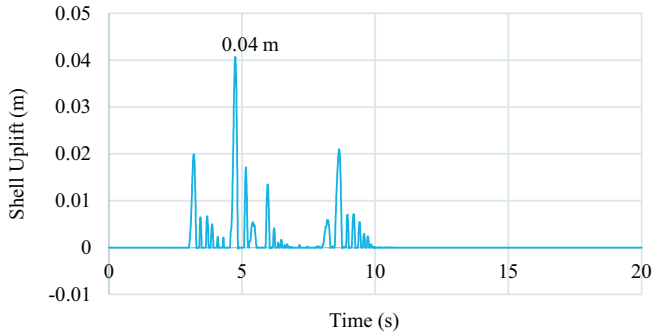

(a)

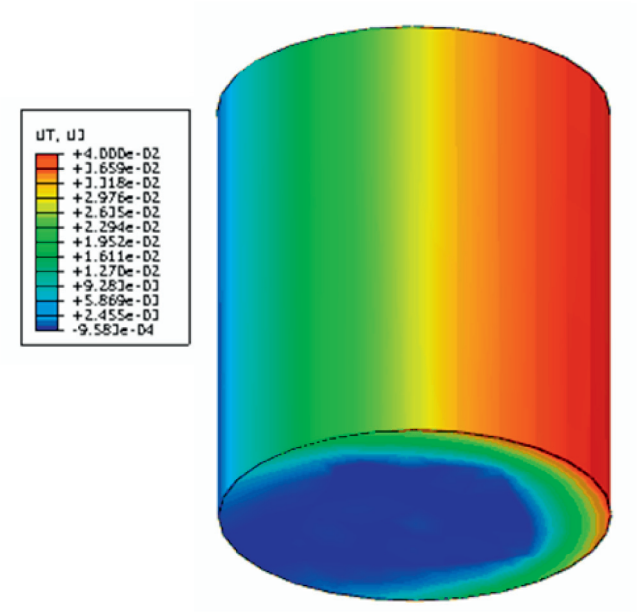

(b)

Fig. 12. Uplift response of the tank a) time-history of the tank uplift b) contour plot of the uplifted tank.

tank.

In order to get a better idea about the uplift behavior of studied tank, IDA analysis was performed using the recorded earthquake in Chalanchulan station. Fig. 13 shows uplift variations in terms of PGA. As shown in this Figure, the threshold PGA for the tank uplift

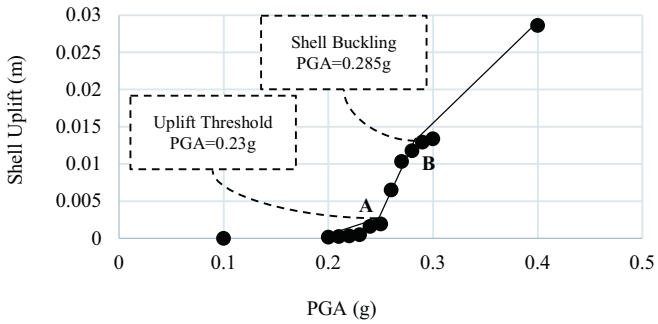

Fig. 13. Variation of the tank uplift with PGA.

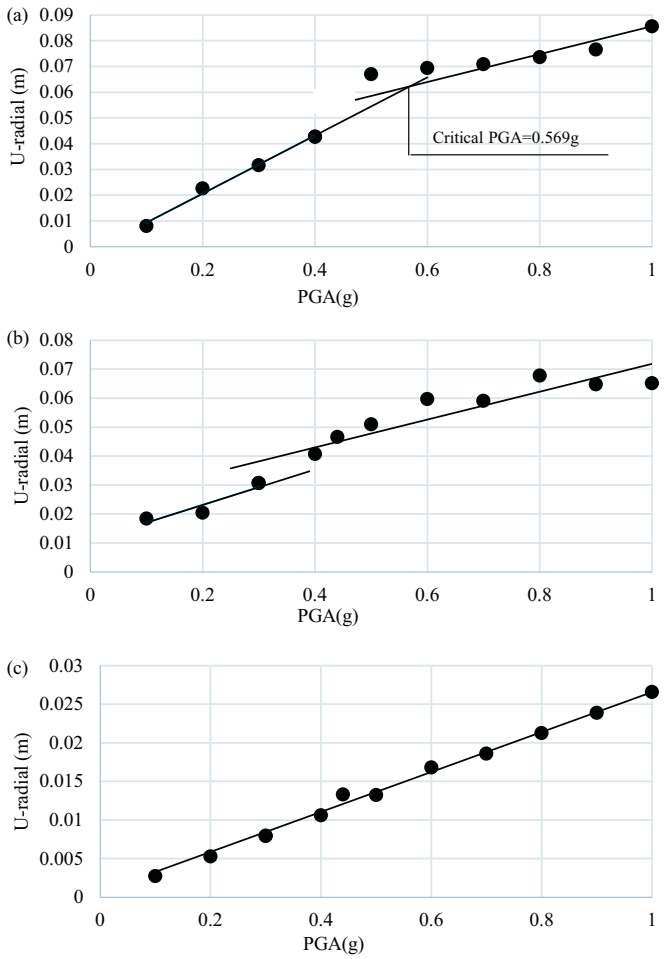

Fig. 14. Pseudo-equilibrium path for critical node of the finite element model. a) %full = 70% b) %full = 50% c) %full = 30%.

is 0.23g. In other words, if the maximum acceleration of the input earthquake were less than 0.2g, the tank uplift would not be probable.

Fig. 13 also shows that in PGA of 0.285g in which shell buckling occurred, the rate of variation of tank uplift by PGA is changed. Such a result seem to indicate that the shell buckling may change the general behavior of tank.

7. Parametric studies

In order to get a better idea about the seismic performance of the considered tank, parametric studies were performed. Generally, amount of stored liquid is one of the most important factors affecting the seismic vulnerability of tanks. On the other hand, shell imperfections play an important role in tank buckling. Hence, in this study the effect of relative amount of stored liquid (%full) and amplitude of shell imperfections on seismic performance of the damaged tank were considered.

7.1. The effect of relative amount of liquid

In order to investigate the effect of %full on seismic performance of the considered tank, relative amounts of liquid of 0, 30%, 50%, 70% and 90% were considered for T3 tank. The incremental dynamic analysis were carried out for each case using the accelerogram of the Silakhor earthquake recorded at Chalanchulan station. Finally, the PGA_{cr} and tank uplift were calculated based on IDA. Fig. 14 shows the pseudo-equilibrium path for the tank with various amounts of stored liquid. As shown in Fig. 14, decreasing the %full from 90% to 70% increases the PGA_{cr} from 0.285g to 0.569g. By decreasing the %full to 50% or less, the paths become almost parallel (Fig. 14b), or fundamentally only one path is formed, and the intersection point does not form at a probable PGA range (Fig. 14c). In other words, in these amounts of stored liquid, buckling is not practically possible in reasonable range of peak ground accelerations.

Fig. 15 shows the variation of the maximum tank uplift with relative amount of stored liquid. As illustrated in this Figure, if the

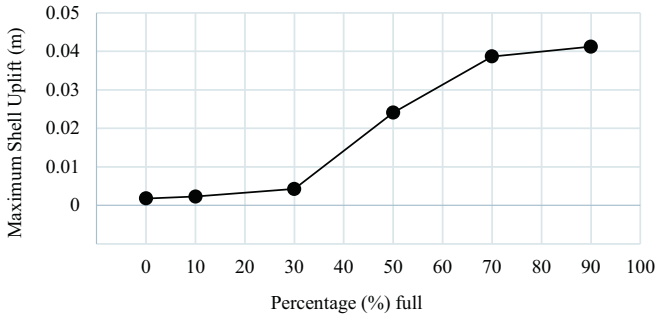

Fig. 15. The effect of relative amount of stored liquid on maximum shell uplift.

amount of stored liquid is equal to or less than 30%, the uplift tank uplift would not be probable. Furthermore, by increasing the %full from 30% to 90%, the shell uplift increases gradually.

7.2. The effect of shell imperfections

Generally, the buckling capacity of cylindrical shells is dependent to shell imperfections. Imperfections are unavoidable characteristics of cylindrical tanks, which happens because of various reasons. One of the most important sources imperfection in steel cylindrical tanks are lap joint imperfections. Lap joint imperfections are local imperfections, which happen because of conventional fabrication process of tanks. The conventional method of fabrication of cylindrical tanks, is rolling flat sheets into curved panels and joining them into complete strakes and mounting the strakes using groove welds [28]. As a result of welding process at lap joints, local imperfections (so-called lap joint imperfections) which are close to axisymmetric are appear. Herein, the effect of lap joint imperfections are taken into account. The amplitude of lap joint imperfections is highly dependent to the construction and can be calculated according to [28,29].

In order to evaluate the effect of lap joint imperfections on PGA_{cr}, three amplitudes of imperfection (W_0 = 3 mm, 4.5 mm and 6 mm) were considered in the FEM model of the tank. IDA analyses were conducted to estimate the critical PGA of each imperfect tank. The critical PGAs corresponding to various imperfection amplitudes are listed in Table 3. Furthermore, the pseudo-equilibrium path of the perfect tank (W_0 = 0) and the worst case of imperfect tanks (W_0 = 6 mm) is compared in Fig. 16. As listed in Table 3, lap joint imperfections can reduce the critical PGA of the tank shell as low as 0.26 g. On the other hand, the critical PGA of the studied tank is not susceptible to the amplitude of imperfection. It should be noted that, such a performance has happened in a particular tank-earthquake case and cannot be generalized to other cases.

8. Conclusions

During the March 31, 2006, seismic event in Silakhor (Iran), some of the un-anchored cylindrical steel storage fuel tanks were damaged. In this study, the failure analysis was performed on one of the damaged tanks. To this end, the uplift and buckling of the inspected tank was carried out using the quasi-static relations as well as inelastic response history analysis using the accelerograms recorded close to the inspected tank.

The uplifting behavior and shell buckling estimated by the FEM model were generally in consistence with actual performance of damaged tank observed during the field investigation. In addition, the location of buckled portion in the model and the actual tank were the same. In other words, the finite element model of inspected tank was capable of estimating the actual performance of the tank during the happened earthquake.

Based on the analyses, the calculated uplift value using numerical analysis is approximately four times the estimations of the quasi-static relations. Neglecting the effects of large deformations and dynamic characteristics of response of the tank to the earthquake in quasi-static approaches would be the main reasons for such a difference.

It was also shown that by reducing the amount of contents, the critical PGA decreases. In tanks with relative amount of contents of 50% or less, the buckling did not occur within the range of maximum acceleration less than 1 g. The results also illustrated that the uplift threshold PGA was 0.23g for the studied tank. Additionally, the rate of variations of the uplift in terms of PGA will change after the shell buckling. In other words, the shell buckling may affect the overall behavior of the tank. Furthermore, consideration of lap joint imperfections in tank shell led to reduction of about 10% in critical PGA.

Table 3
The critical PGA of perfect and imperfect tank shells.

	W_0 = 0	W_0 = 3 mm	W_0 = 4.5 mm	W_0 = 6 mm
$PGA_{cr\ (g)}$	0.285	0.258	0.257	0.256

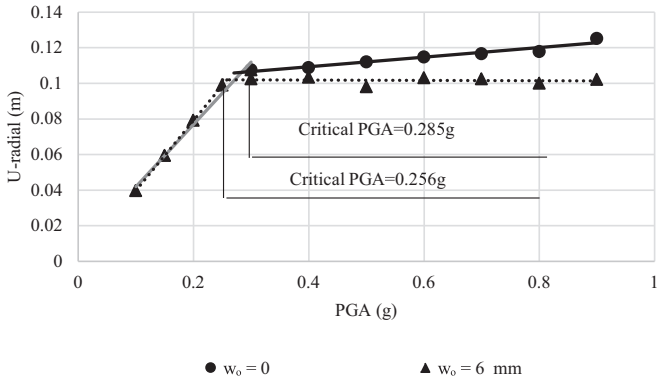

Fig. 16. The Comparison of the Pseudo-equilibrium paths for perfect ($w_0 = 0$) and imperfect ($w_0 = 6$ mm) tanks.

Declarations of interest

None.

References

[1] O.R. Jaiswal, D.C. Rai, S.K. Jain, Review of seismic codes on liquid-containing tanks, Earthquake Spectra 23 (1) (2007 Feb) 239–260.
[2] H. Sezen, A.S. Whittaker, Seismic performance of industrial facilities affected by the 1999 Turkey earthquake, J. Perform. Constr. Facil. 20 (1) (2006 Feb) 28–36.
[3] S. Eshghi, M.S. Razzaghi, Performance of industrial facilities in the 2003 Bam, Iran, earthquake, Earthquake Spectra 21 (S1) (2005 Dec) 395–410.
[4] S. Eshghi, M.S. Razzaghi, Performance of cylindrical liquid storage tanks in Silakhor, Iran earthquake of March 31, 2006, Bulletin of the New Zealand Society for Earthquake Engineering. 40 (4) (2007 Dec).
[5] M.S. Razzaghi, S. Eshghi, Probabilistic seismic safety evaluation of precode cylindrical oil tanks, J. Perform. Constr. Facil. 29 (6) (2014 Sep 26) 04014170.
[6] M. Rahnama, G. Morrow, Performance of industrial facilities in the August 17, Izmit Earthquake. Proceedings of the 12WCEE, Paper. 2000 Jan (2851), 1999.
[7] H. Akatsuka, H. Kobayashi, Fire of Petroleum Tank, Etc. by Niigata Earthquake. Failure Knowledge Database, Japan Science and Technology Agency, (2008).
[8] H.N. Phan, F. Paolacci, S. Alessandri, Fragility analysis methods for steel storage tanks in seismic prone areas. In ASME, Pressure Vessels and Piping Conference 2016 Jul 17 (pp. V008T08A023-V008T08A023), American Society of Mechanical Engineers, 2016.
[9] P. Malhotra, Practical nonlinear seismic analysis of tanks, Earthquake Spectra 16 (2) (2000 May) 473–492.
[10] M.N. Ahari, S. Eshghi, M.G. Ashtiany, The tapered beam model for bottom plate uplift analysis of unanchored cylindrical steel storage tanks, Eng. Struct. 31 (3) (2009 Mar 1) 623–632.
[11] M.J. O'Rourke, P. So, Seismic fragility curves for on-grade steel tanks, Earthquake Spectra 16 (4) (2000 Nov) 801–815.
[12] BHRC. Silakhor Earthquake on, Building and Housing Research Center. (March 31, 2006) 2006 http://bhrc.ac.ir.
[13] ABAQUS Explicit User Manual, Version 6.4. Hibbit, Karlsson and Sorensen, (2002).
[14] O. Curadelli, Equivalent linear stochastic seismic analysis of cylindrical base-isolated liquid storage tanks, J. Constr. Steel Res. 83 (2013 Apr 1) 166–176.
[15] J.C. Virella, L.E. Suarez, L.A. Godoy, Effect of pre-stress states on the impulsive modes of vibration of cylindrical tank-liquid systems under horizontal motions, Modal Analysis. 11 (9) (2005 Sep) 1195–1220.
[16] H.M. Koh, J.K. Kim, J.H. Park, Fluid–structure interaction analysis of 3-D rectangular tanks by a variationally coupled BEM–FEM and comparison with test results, Earthquake Engineering & Structural Dynamics 27 (2) (1998 Feb) 109–124.
[17] Y.L. Young, Fluid–structure interaction analysis of flexible composite marine propellers, Journal of Fluids and Structures 24 (6) (2008 Aug 1) 799–818.
[18] H.M. Westergaard, Water pressures on dams during earthquakes, Trans. Am. Soc. Civ. Eng. 98 (1933) 418–433.
[19] J.M. Rotter, Local collapse of axially compressed pressurized thin steel cylinders, J. Struct. Eng. 116 (7) (1990 Jul) 1955–1970.
[20] NZSEE. Seismic Design of Storage Tanks, New Zealand National Society for Earthquake Engineering, New Zealand. Second edition, Wellington, 2009.
[21] European Committee for Standardization - CEN. Eurocode 8: Design of Structures for Earthquake Resistance - Part 4: Silos, Tanks and Pipelines, (2006).
[22] B. Budiansky, R.S. Roth, Axisymmetric dynamic buckling of clamped shallow spherical shells. (1962) 597–606 Dec.
[23] B. Budiansky, Dynamic buckling of elastic structures: criteria and estimates, Dynamic Stability of Structures, 1967, pp. 83–106.
[24] N. Buratti, M. Tavano, Dynamic buckling and seismic fragility of anchored steel tanks by the added mass method, Earthquake Engineering & Structural Dynamics 43 (1) (2014 Jan 1) 1–21.
[25] J.C. Virella, L.A. Godoy, L.E. Suárez, Dynamic buckling of anchored steel tanks subjected to horizontal earthquake excitation, J. Constr. Steel Res. 62 (6) (2006 Jun 1) 521–531.
[26] M.R. Maheri, A. Abdollahi, The effects of long-term uniform corrosion on the buckling of ground based steel tanks under seismic loading, Thin-Walled Struct. 62 (2013 Jan 1) 1–9.
[27] F.J. Cambra, Earthquake response considerations of broad liquid storage tanks, NASA STI/Recon Technical Report N. (1982 Nov) 84.
[28] J.G. Teng, J.M. Rotter (Eds.), Buckling of Thin Metal Shells, CRC Press, London, 2006.
[29] ENV 1993-1-6, Eurocode 3: Design of Steel Structures, Part 1.6: General Rules – Supplementary Rules for the Strength and Stability of Shell Structures, Eurocode 3 Part 1.6, CEN, Brussels, (1999).